The Role of Astrocytes in Alzheimer's Disease Progression

Swadesh Pal[1] and Roderick Melnik[1,2(✉)]

[1] M3AI Laboratory, MS2Discovery Interdisciplinary Research Institute, Wilfrid Laurier University, Waterloo, ON N2L 3C5, Canada
rmelnik@wlu.ca
[2] BCAM - Basque Center for Applied Mathematics, 48009 Bilbao, Spain
http://m3ai.wlu.ca

Abstract. Astrocytes are a particular type of glial cells observed throughout the gray matter in the brain. In a healthy brain, they help to defend evolutionarily conserved astrogliosis programs and maintain neuronal metabolism. On the other hand, in the Alzheimer's disease (AD) affected brain, they release neurotoxins because of the adopting behaviours of different functions depending on the disease progression. Along with astrocytes, amyloid-beta (Aβ) and tau proteins (τP) play a prominent role in AD. In this paper, we have developed a model and have studied the dual action of astrocytes with Aβ, τP, and their toxic forms in the brain connectome. Initial conditions-dependent solutions of the model demonstrate that the treatment depends on AD's status at the first diagnosis time. With an increase in the clearance rate of toxic Aβ by the astrocytes, the model predicts a cure possibility from AD. Furthermore, the network model with non-uniform parameter values in different regions, developed here, provides a better insight into the distributions of the concentrations in the brain connectome.

Keywords: Alzheimer's disease · Brain connectome · Data-driven models · Cell interactions · Bistability and bifurcation · Amyloid-beta · Tau protein · Astrocytes · Network models

1 Introduction

Alzheimer's disease (AD) is one of the leading neurodegenerative diseases nowadays. AD causes neuronal death in the brain and disables different functional abilities. According to the Alzheimer's Association, more than 50 million people worldwide have this dementia, and it is expected to reach over 150 million in three decades [1]. AD develops very slowly in the brain at the early stage, and it is hard to identify such changes. That is one of the main reasons for the AD progression to be detected and analyzed. Numerous studies have been carried out to determine the mechanism behind AD progression, but still, it is not fully clear. As of today, only four drugs are approved by the Food and Drug Administration

I. Rojas et al. (Eds.): IWBBIO 2022, LNBI 13346, pp. 47–58, 2022.
https://doi.org/10.1007/978-3-031-07704-3_5

(FDA) for AD treatments. Moreover, the approved drugs do not prevent the neuronal loss, although they do help in symptoms management [2]. Therefore, disease-modifying therapies play an important role in controlling the brain's AD progression.

It is well accepted that the amyloid-beta (Aβ) and tau protein (τP) are the two main ingredients in developing the AD [3,4]. Aβ is accumulated in the extracellular space and deposited in the form of insoluble plaques. On the other hand, τP forms neurofibrillary tangles (NFT) inside the brain cells. Significant production of plaques and NFTs disrupt the normal activities of the brain cell and move towards AD.

Astrocytes perform various functions in the brain, and their abnormality causes multiple neurodegenerative diseases, e.g., AD, Parkinson's disease [5,6]. They release gliotransmitters in different brain regions and help in the modulation of memory and learning processes [7–9]. Earlier research suggested that the astrocytes clear the plaques from the brain cells and keep them healthy. But, a significant production of plaque interrupts the astrocyte's functions; as a result, AD develops in the brain [10]. Glutamate NMDA in astrocytes is the most popular receptor in the physiopathology of AD, and it interferes in neuronal-glial signaling [11,12]. The difference between neuronal and glial NMDA receptor signals in astrocytes provides a better understanding of the therapy's development in AD prevention and control.

In this work, we introduce the astrocyte's interaction with Aβ and τP and their toxic forms. We use the heterodimer model in the reaction kinetics to describe the interaction between amyloid-beta and tau proteins [13,14]. In the modified model, we introduce the clearance of toxic Aβ by the astrocytes, and the astrocytes follow the Allee type dynamics. Moreover, we formulate a network mathematical model to integrate the brain connectome data and examine the effect of the parameter involved in the Aβ clearance term. The AD status at the first treatment is also dependent on the AD progression. Therefore, we have also studied the solution depending on the initial conditions.

The organization of the rest of this paper is as follows. In Sect. 2, we describe the reaction-diffusion model and the network model. Simulation results are presented in Sect. 3 followed by conclusions in Sect. 4.

2 Models for AD

We consider $\Omega \subset \mathbb{R}^3$ is a spatial domain. For $\mathbf{x} \in \Omega$ and time $t \in \mathbb{R}^+$, we denote by $u = u(\mathbf{x}, t)$ and $v = v(\mathbf{x}, t)$, the concentrations of healthy Aβ and τP, respectively. Similarly, we denote by $\widetilde{u} = \widetilde{u}(\mathbf{x}, t)$ and $\widetilde{v} = \widetilde{v}(\mathbf{x}, t)$, the concentrations of toxic Aβ and τP, respectively. The evolution of concentrations of the four populations can then be given as follows [13,15]:

$$\frac{\partial u}{\partial t} = \nabla \cdot (\mathbf{D}_u \nabla u) + a_0 - a_1 u - a_2 u\widetilde{u}, \tag{1a}$$
$$\frac{\partial \widetilde{u}}{\partial t} = \nabla \cdot (\mathbf{D}_{\widetilde{u}} \nabla \widetilde{u}) - \widetilde{a}_1 \widetilde{u} + a_2 u\widetilde{u}, \tag{1b}$$
$$\frac{\partial v}{\partial t} = \nabla \cdot (\mathbf{D}_v \nabla v) + b_0 - b_1 v - b_2 v\widetilde{v} - b_3 \widetilde{u} v\widetilde{v}, \tag{1c}$$
$$\frac{\partial \widetilde{v}}{\partial t} = \nabla \cdot (\mathbf{D}_{\widetilde{v}} \nabla \widetilde{v}) - \widetilde{b}_1 \widetilde{v} + b_2 v\widetilde{v} + b_3 \widetilde{u} v\widetilde{v}, \tag{1d}$$

with non-negative initial conditions and no-flux boundary conditions. Here, the first two equations correspond to the usual heterodimer model for the healthy and toxic variants of the protein u and the last two equations are the same for v. The parameters a_0 and b_0 are the mean production rates of healthy proteins, $a_1, b_1, \widetilde{a}_1$ and $\widetilde{b}_1$ are the mean clearance rates of healthy and toxic proteins, and a_2 and b_2 represent the mean conversion rates of healthy proteins to toxic proteins. The parameter b_3 is the coupling between the two proteins $A\beta$ and τP. The first term in the right-hand side in all equations represent the diffusion tensors.

Astrocytes are present in the brain cells, and generally, they remain inactive till a sufficient accumulation of sticky protein (toxic amyloid-beta) in the brain. At the initial stage, brain cells send indications through which astrocytes start accumulations. After reaching a peak density, astrocytes damage the toxic amyloid-beta [16]. Here, we introduce such type of dynamics of astrocytes (by modifying $\widetilde{u}$), the above system (1) as follows:

$$\frac{\partial u}{\partial t} = \nabla \cdot (\mathbf{D}_u \nabla u) + a_0 - a_1 u - a_2 u\widetilde{u}, \tag{2a}$$
$$\frac{\partial \widetilde{u}}{\partial t} = \nabla \cdot (\mathbf{D}_{\widetilde{u}} \nabla \widetilde{u}) - \widetilde{a}_1 \widetilde{u} + a_2 u\widetilde{u} - \alpha w\widetilde{u}, \tag{2b}$$
$$\frac{\partial v}{\partial t} = \nabla \cdot (\mathbf{D}_v \nabla v) + b_0 - b_1 v - b_2 v\widetilde{v} - b_3 \widetilde{u} v\widetilde{v}, \tag{2c}$$
$$\frac{\partial \widetilde{v}}{\partial t} = \nabla \cdot (\mathbf{D}_{\widetilde{v}} \nabla \widetilde{v}) - \widetilde{b}_1 \widetilde{v} + b_2 v\widetilde{v} + b_3 \widetilde{u} v\widetilde{v}, \tag{2d}$$
$$\frac{\partial w}{\partial t} = \nabla \cdot (\mathbf{D}_w \nabla w) + w(c_0 - c_1 w)(w - \widetilde{u}). \tag{2e}$$

The second term in the right-hand side of the last equation of (2) represents the growth or decay of astrocytes. In the absence of toxic amyloid-beta, astrocytes increase their concentration and are saturated at c_0/c_1. If $w > \widetilde{u}$, then the term contributes to its growth and helps to decrease the toxic amyloid-beta levels. On the other hand, for $w < \widetilde{u}$, it drives the concentration of astrocytes to decay to 0. The last term in the right-hand side of the second equation of (2) represents the clearance of toxic Aβ by astrocytes. This signifies that astrocytes can cure up to a certain level of toxic load in the brain, and after that, astrocytes can not decrease the toxic load, rather it helps in building the AD. The failing case does not contribute to the clearance of toxic Aβ. Hence, it supports increasing the toxic

Aβ concentration indirectly, and we call this as the astrocytes' activated stage. We analyze the role of astrocytes results with the help of numerical simulations.

2.1 Network Model for the Brain Connectome

Here, we formulate the network mathematical model corresponding to the modified model (2) for the brain connectome data [13,14,17]. Suppose, the brain data is represented by a graph $\mathcal{G}$ with V nodes and E edges. For the graph $\mathcal{G}$, we construct the adjacency matrix $\mathbf{A}$. This helps us to construct the Laplacian in the graph. We define the (i,j) $(i,j=1,2,3,\ldots,V)$ element of the matrix $\mathbf{A}$ as

$$A_{ij} = \frac{n_{ij}}{l_{ij}^2},$$

where n_{ij} is the mean fiber number and l_{ij}^2 is the mean length squared between the nodes i and j. Now, we define the elements of the Laplacian matrix $\mathbf{L}$ as

$$L_{ij} = \rho(D_{ii} - A_{ij}), \quad i,j = 1,2,3,\ldots,V,$$

where ρ is the diffusion coefficient and $D_{ii} = \sum_{j=1}^{V} A_{ij}$ are the elements of the diagonal weighted-degree matrix. With the help of the Laplacian matrix, we derive a network mathematical model on the graph $\mathcal{G}$, whose dynamics at each node is given by

$$\frac{du_j}{dt} = -\sum_{k=1}^{V} L_{jk}^{u} u_k + a_0 - a_1 u_j - a_2 u_j \widetilde{u}_j, \tag{3a}$$

$$\frac{d\widetilde{u}_j}{dt} = -\sum_{k=1}^{V} L_{jk}^{\widetilde{u}} \widetilde{u}_k - \widetilde{a}_1 \widetilde{u}_j + a_2 u_j \widetilde{u}_j - \alpha w_j \widetilde{u}_j, \tag{3b}$$

$$\frac{dv_j}{dt} = -\sum_{k=1}^{V} L_{jk}^{v} v_k + b_0 - b_1 v_j - b_2 v_j \widetilde{v}_j - b_3 \widetilde{u}_j v_j \widetilde{v}_j, \tag{3c}$$

$$\frac{d\widetilde{v}_j}{dt} = -\sum_{k=1}^{V} L_{jk}^{\widetilde{v}} \widetilde{v}_k - \widetilde{b}_1 \widetilde{v}_j + b_2 v_j \widetilde{v}_j + b_3 \widetilde{u}_j v_j \widetilde{v}_j, \tag{3d}$$

$$\frac{dw_j}{dt} = -\sum_{k=1}^{V} L_{jk}^{w} w_k + w_j(c_0 - c_1 w_j)(w_j - \widetilde{u}_j), \tag{3e}$$

where u_j, $\widetilde{u}_j$, v_j, $\widetilde{v}_j$, and w_j denote the concentrations of Aβ, toxic Aβ, τP, toxic τP and astrocytes, respectively, at the node j. In the simulations, we have used non-negative initial conditions for all the variables.

2.2 Homogeneous System for the Network Model

The homogeneous system corresponding to the model (3) can be obtained by assuming the independence of spatial terms. This allows us to focus on the dynamics of AD propagations. Therefore, in this case, the system (3) reduces to

$$\frac{du}{dt} = a_0 - a_1 u - a_2 u\widetilde{u}, \tag{4a}$$

$$\frac{d\widetilde{u}}{dt} = -\widetilde{a}_1\widetilde{u} + a_2 u\widetilde{u} - \alpha w\widetilde{u}, \tag{4b}$$

$$\frac{dv}{dt} = b_0 - b_1 v - b_2 v\widetilde{v} - b_3\widetilde{u}v\widetilde{v}, \tag{4c}$$

$$\frac{d\widetilde{v}}{dt} = -\widetilde{b}_1\widetilde{v} + b_2 v\widetilde{v} + b_3\widetilde{u}v\widetilde{v}, \tag{4d}$$

$$\frac{dw}{dt} = w(c_0 - c_1 w)(w - \widetilde{u}), \tag{4e}$$

with non-negative initial conditions for all the variables. The model (4) provides us with a better us into the disease progression, as we demonstrate in the next section.

3 Results and Discussions

In this section, we analyze the models (3) and (4) numerically. We have adopted the parameter values for the amyloid-beta and tau protein interactions from [13]. Further, we have integrated the brain connectome data (freely available on https://braingraph.org [18]) in the network model. An in-house tool based on Matlab and C-language has been used for the simulations. We have used the SHARCNET (www.sharcnet.ca) high performance computational facilities to minimize the time in computations.

To date, AD treatment is still only symptomatic. As mentioned earlier, four drugs have been approved by the Food and Drug Administration (FDA) to treat AD. They help only in the symptoms' management, not to prevent any neuronal damage in the brain [2]. Due to the inefficacy of the drugs, researchers target the pathological features of the disease. Amyloid-beta and tau protein therapies remain the keys to mitigating symptoms from AD. According to the amyloid-beta hypothesis, accumulation of Aβ peptide, aggregation, and deposition in the form of Aβ plaques is the main reason for AD. Researchers studied different anti-amyloid therapies to slow down the AD progression in the brain.

Here, we focus on toxic Aβ and toxic τP clearances. For the toxic Aβ clearance, we increase the parameter values of α. On the other hand, we decrease the parameter values of b_3 in some parts of the brain connectome to account for the toxic τP clearance. We expect less toxic loads in the brain connectome in both the clearances, so that minor damage occur in the brain cells.

Depending on the parameter values, the homogeneous system (4) has many non-trivial equilibrium points. One may find those equilibrium points algebraically by solving the homogeneous system with taking the derivative terms as zero. We list two of them as $E_0 = (u_0, \widetilde{u}_0, v_0, \widetilde{v}_0, w_0) = (a_0/a_1, 0, b_0/b_1, 0, 0)$ and $E_1 = (u_1, \widetilde{u}_1, v_1, \widetilde{v}_1, w_1) = (a_0/a_1, 0, b_0/b_1, 0, c_0/c_1)$ and we find the other equilibrium points numerically later in this section. The equilibrium point E_1 is the healthy state as it has zero toxic loads with non-zero astrocytes' concentration. If the equilibrium component corresponding to astrocytes is larger than

the toxic amyloid beta and zero toxic loads of tau protein, then the equilibrium point is healthy; otherwise it is a disease state. Here, we analyze the disease development by varying some parameter values and different initial conditions, known as the initial stage of the treatment.

3.1 Focussing on the Dynamics of AD Propagation

In this section, we study the behaviour of the solutions of the system (4). We first consider the parameter α, the clearance by the astrocytes. All the fixed parameters are chosen from the Table 1 except the parameter α. These parameters are corresponding to the secondary tauopathy, studied earlier in [13–15] in the absence of astrocytes. For the primary tauopathy, amyloid-beta does not alter the onset of the regional pathology. We have considered the mixture of primary and secondary tauopathies parameters in the coming section. For $\alpha \in [0.1, 0.3]$, the total number of equilibrium points of the homogeneous system varies. But, for all the cases, two of them are locally asymptotically stable, and the rest are unstable.

Table 1. Fixed parameters values [13].

Parameter	Value	Parameter	Value	Parameter	Value	Parameter	Value
a_0	1.035	a_1	1.38	a_2	1.38	$\widetilde{a}_1$	0.828
b_0	0.69	b_1	1.38	b_2	1.035	$\widetilde{b}_1$	0.552
c_0	1.0	c_1	1.0	b_3	4.14	α	0.2

We fix $\alpha = 0.1$. The stable equilibrium points of the system (4) corresponding to $\alpha = 0.1$ are $(u_1^s, \widetilde{u}_1^s, v_1^s, \widetilde{v}_1^s, w_1^s) = (0.6, 0.25, 0.27, 0.58, 0)$ and $(u_2^s, \widetilde{u}_2^s, v_2^s, \widetilde{v}_2^s, w_2^s) = (0.75, 0.007, 0.5, 0, 1)$. Both the stable equilibrium points represent the disease state due to the non-zero concentrations of toxic amyloid-beta and tau proteins. Depending on the initial conditions, the solution of the homogeneous system (4) converges to one of these stable equilibrium points. We plot their basin of attractions for different values of α in Fig. 1. In the simulations, we fix the initial conditions for u, v and $\widetilde{v}$ as a_0/a_1, b_0/b_1 and 0.05, respectively, and we vary $\widetilde{u}$ and w from 0.01 to 0.49 with all possible combinations. While it is possible to analyze the situation with a higher range in the initial conditions for $\widetilde{u}$ and w, but the mentioned range is sufficient for the goal of this paper. The solutions of the homogeneous system (4) with the initial condition region below the curve $\alpha = 0.1$ converge to $(u_1^s, \widetilde{u}_1^s, v_1^s, \widetilde{v}_1^s, w_1^s)$ while the solution for the upper region converges to the other stable equilibrium point.

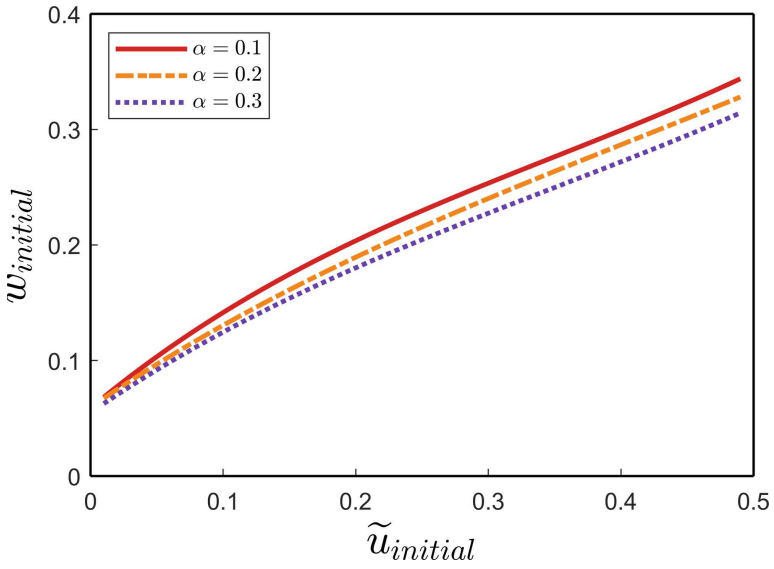

Fig. 1. Bifurcation curve which separates the basin of attractions of two stable equilibrium points for the homogeneous system with different values of α. (Color figure online)

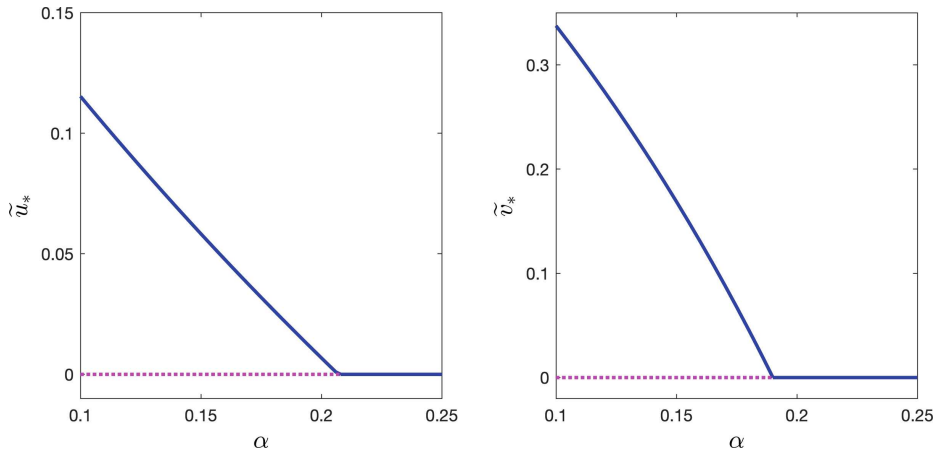

Fig. 2. Transcritical bifurcations of the equilibrium points of the homogeneous system (4). (Color figure online)

The equilibrium point $(u_1^s, \widetilde{u}_1^s, v_1^s, \widetilde{v}_1^s, w_1^s)$ has high concentrations of toxic amyloid-beta and toxic tau protein compared to the other stable equilibrium point. Hence, the solutions of the homogeneous system converge to the more disease state if the initial conditions are chosen from the lower region compared to the upper region, of the partition curve. With an increase in the parameter values α, the partition curves for the basin of attractions of the stable equilibrium points shift downwards. We observe that, for $\alpha = 0.3$, the solutions in the lower region converges to the disease state whereas the solution in the upper region converges to the healthy state. Therefore, the temporal model predicts that, with an increase in the damage rate of the toxic amyloid-beta by the astrocytes can

control the AD propagation in the brain. However, we verify this observation with the help of the network model (3) defined on the brain connectome for uniform and non-uniform parameter values in different brain regions.

Figure 2 depicts the two subcritical transcritical bifurcations occur at $\alpha = 0.192$ and $\alpha = 0.208$. Here, we have shown only the bifurcation of one stable equilibrium point, and the other stable equilibrium point does not exhibit any such type of bifurcation in the mentioned range. As we see, for $0.192 < \alpha < 0.208$, a non-zero concentration corresponding to the toxic Aβ exists. In this case, both the stable equilibrium points correspond to the disease state. For $\alpha > 0.208$, both the toxic concentrations become zero; hence, a healthy stable equilibrium occurs of the system (4).

3.2 AD Propagation in the Brain Connectome

Here, we integrate the brain connectome data and investigate the solution behaviours of the network model (3). The integrated brain connectome data consists of $V = 1015$ nodes and $E = 16,280$ edges. First, we set uniform parameter values [see Table 1] for all the regions in the brain connectome. We choose the diffusion coefficients for u, $\widetilde{u}$, v, $\widetilde{v}$ and w as 1.38, 0.138, 1.38, 0.014 and 1.38, respectively, and these are fixed throughout the paper (adopted from [13,14]). For all the nodes in the brain connectome, the chosen initial conditions for u, v and w are a_0/a_1, b_0/b_1 and 0.05, respectively.

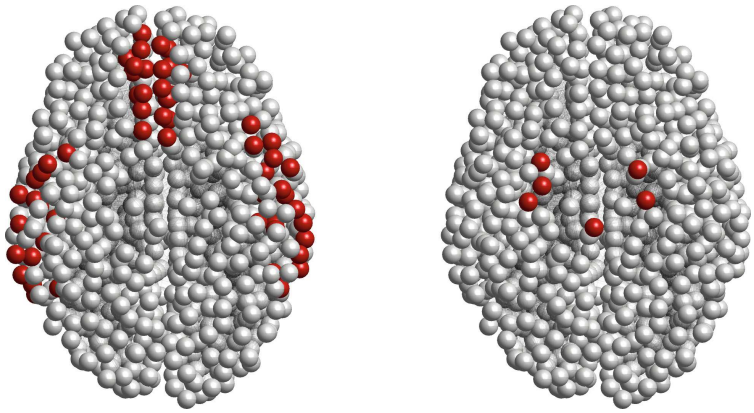

Fig. 3. Initial seeding sites for the toxic amyloid-beta and toxic tau proteins in the brain connectome. Red colors represent the non-zero concentration and gray colors represent the zero concentration. (Color figure online)

The initial seeding sites for the toxic amyloid-beta in the brain connectome are the temporobasal and frontomedial regions. On the other hand, the initial seeding sites for the toxic tau proteins are the locus coeruleus and transentorhinal associated regions [see Fig. 3]. The toxic loads for amyloid-beta and tau proteins

are 0.0375 and 0.0125, respectively, and these non-zero concentrations are the 5% of the healthy concentrations. We use these initial conditions for the rest of the paper.

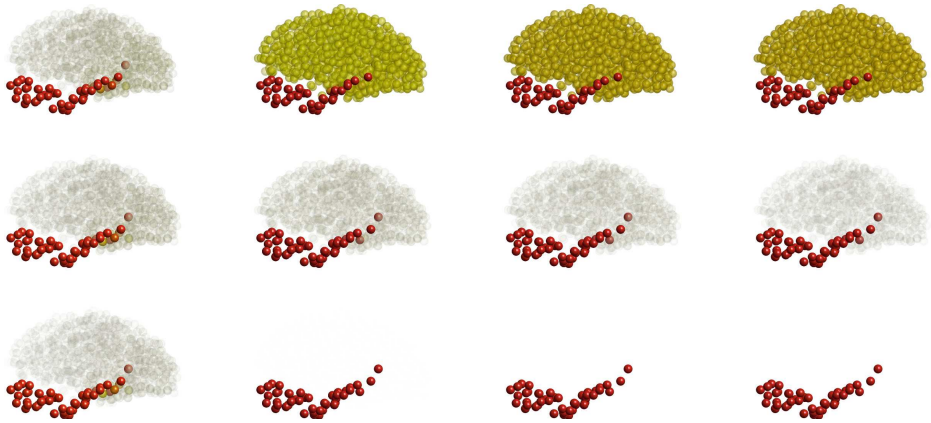

Fig. 4. Distributions of toxic amyloid-beta in the brain connectome for the network model at different time steps with different values of α. Top, middle and bottom panels are corresponding to $\alpha = 0.1, 0.2$ and 0.3. Left to right is corresponding to $t = 20, 50, 70$ and 120 for top to bottom panels. Red colors represent the high concentration, and gray colors represent the low concentration. (Color figure online)

We plot the simulation results for the network model corresponding to the toxic amyloid-beta in Fig. 4 for three different values of α. For $\alpha = 0.1$, we see the top panel in Fig. 4, some nodes converge to one steady-state, and the rest converge to the other. This bistability occurs in the network model due to two stable equilibrium points for the homogeneous system. With an increase in the parameter associated with the death of toxic amyloid-beta due to astrocytes, less toxic concentrations distribute in the brain connectome. Hence, minor damage occurs in the brain.

Now, we move forward to the case of non-uniform parameter values in the brain connectome. We use the general synthetic parameters values mentioned in Table 1 with some modifications in the parameters b_2 and b_3 in some regions of the brain connectome. The modified parameter values are mentioned in Tables 2 and 3. We observe that the solution corresponding to the toxic tau protein $\widetilde{v}$ converges to the different steady states at different nodes in the brain connectome [see Fig. 5]. The non-uniform distribution of 18F-AV-1451 radiotracer has been observed in [19].

Table 2. Modified b_3 parameter values in different regions [13].

Brain region and modified b_3 value			
Pars Opercularis	7.452	Rostral middle frontal gyrus	6.707
Superior frontal gyrus	7.452	Caudal middle frontal gyrus	7.452
Precentral gyrus	5.589	Postcentral gyrus	3.726
Lateral orbitofrontal cortex	6.486	Medial orbitofrontal cortex	6.486
Pars triangularis	5.520e-6	Rostral anterior cingulate	6.210e-6
Posterior cingulate cortex	3.45	Inferior temporal cortex	13.11
Middle temporal gyrus	11.04	Superior temporal sulcus	8.97
Superior temporal gyrus	8.28	Superior parietal lobule	12.42
Cuneus	13.8	Pericalcarine cortex	13.8
Inferior parietal lobule	11.73	Lateral occipital sulcus	15.18
Lingual gyrus	13.8	Fusiform gyrus	7.59
Parahippocampal gyrus	11.04	Temporal pole	1.104e-5

The non-zero steady-state corresponding to the toxic amyloid-beta does not depend on the parameters b_2 or b_3. Hence, the solution corresponding to toxic amyloid-beta remains uniform in most regions. An increase in the clearance rate of the toxic amyloid-beta by the astrocytes (i.e., α) decreases the toxic loads in most brain connectome regions. But, the toxic loads do not become zero for all the areas, i.e., the astrocytes can not clear the full toxic load. So, AD may start to propagate once we decrease the clearance rate, and it would be interesting to see in the future.

Table 3. Modified b_2 and b_3 parameter values in different brain regions [13].

Brain region	Entorhinal cortex	Pallidum	Locus coeruleus	Putamen	Precuneus
b_2	3.125	2.76	1.38	3.795	3.105
b_3	1.104e-5	2.76	1.38	3.795	3.105

We have not considered the clearance of toxic τP separately. Here, the parameter values of b_2 and b_3 are modified in most regions. This was an inherent clearance of toxic τP in the study.

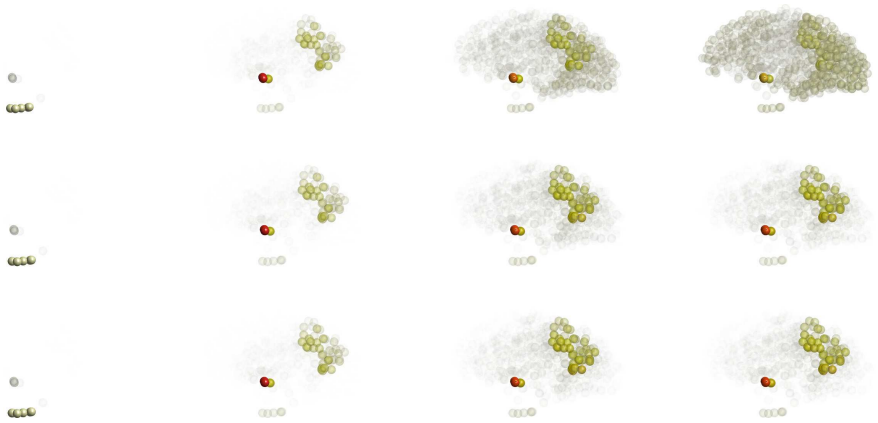

Fig. 5. Distributions of toxic tau protein in the brain connectome for the network model at different time steps with different values of α. Top, middle and bottom panels are corresponding to $\alpha = 0.1, 0.2$ and 0.3. Left to right is corresponding to $t = 20, 50, 70$ and 120 for top to bottom panels. Red colors represent the high concentration, and gray colors represent the low concentration. (Color figure online)

4 Conclusions

In this paper, we have introduced astrocytes' interactions with amyloid-beta and tau proteins and their toxic forms. We have considered a heterodimer model for the amyloid-beta and tau protein interactions [13]. Our modelling approach has allowed us to study the clearance of the toxic amyloid-beta by the astrocytes.

We have observed that the initial conditions play a crucial role in the resulting solutions. Further, with the help of brain connectome data applied to the network model, we have analyzed the AD progression in the brain. With an increase in the clearance rate of the toxic amyloid-beta by the astrocytes, the toxic load in the brain connectome is reduced significantly. This result is unaltered for uniform and non-uniform parameter values in different brain regions. Finally, a non-uniform toxic tau protein distribution in the brain connectome has been observed for different parameter values (related to τP) in distinct areas, confirming a good agreement obtained by the models developed here with experimental results (e.g., [19]). Therefore, the considered model suggests that the clearance of toxic amyloid-beta by astrocytes restricts the amyloid plaque distributions in the whole brain and keeps the brain safe from full-scale AD progression.

Acknowledgements. Authors are grateful to the NSERC and the CRC Program for their support. RM is also acknowledging support of the BERC 2022–2025 program and Spanish Ministry of Science, Innovation and Universities through the Agencia Estatal de Investigacion (AEI) BCAM Severo Ochoa excellence accreditation SEV-2017–0718 and the Basque Government fund AI in BCAM EXP. 2019/00432. This research was enabled in part by support provided by SHARCNET (www.sharcnet.ca) and Digital Research Alliance of Canada (www.alliancecan.ca).

References

1. Alzheimer's Association: 2020 Alzheimer's disease facts and figures. Alzheimer's Dementia, pp. 391–460 (2020)
2. Vaz, M., Silvestre, S.: Alzheimer's disease: recent treatment strategies. Eur. J. Pharmacol. **887**, 173554 (2020)
3. Hardy, J.A., Higgins, G.A.: Alzheimer's disease: the amyloid cascade hypothesis. Science **256**, 184–186 (1992)
4. Götz, J., Halliday, G., Nisbet, R.M.: Molecular pathogenesis of the tauopathies. Annu. Rev. Pathol. **14**, 239–261 (2019)
5. Verkhratsky, A., et al.: Astrocytes in Alzheimer's disease. Neurother. Journal Am. Soc. Exp. Neurother. **7**, 399–412 (2010)
6. Trujillo-Estrada, L., et al.: Astrocytes: from the physiology to the disease. Curr. Alzheimer Res. **16**, 675–698 (2019)
7. Panatier, A., et al.: Glia-derived D-serine controls NMDA receptor activity and synaptic memory. Cell **125**, 775–784 (2006)
8. Ding, S., et al.: Enhanced astrocytic Ca2+ signals contribute to neuronal excitotoxicity after status epilepticusm. J. Neurosci. **27**, 10674–10684 (2007)
9. González-Reyes, R.E., et al.: Involvement of astrocytes in Alzheimer's Disease from a neuroinflammatory and oxidative stress perspective. Front. Mol. Neurosci. **10**, 427 (2017)
10. Rodríguez-Arellano, J.J., et al.: Astrocytes in physiological aging and Alzheimer's disease. Neuroscience **323**, 170–182 (2016)
11. Parameshwaran, K., Dhanasekaran, M., Suppiramaniam, V.: Amyloid beta peptides and glutamatergic synaptic dysregulation. Exp. Neurol. **210**, 7–13 (2008)
12. Mota, S.I., Ferreira, I.L., Rego, A.C.: Dysfunctional synapse in Alzheimer's disease - a focus on NMDA receptors. Neuropharmacology **76**, 16–26 (2014)
13. Thompson, T.B., Chaggar, P., Kuhl, E., Goriely, A.: Protein-protein interactions in neurodegenerative diseases: a conspiracy theory. PLoS Comput. Biol. **16**, e1008267 (2020)
14. Pal, S., Melnik, R.: Nonlocal models in the analysis of brain neurodegenerative protein dynamics with application to Alzheimer's disease. Sci. Rep. **12**, 7328 (2022)
15. Pal, S., Melnik, R.: Pathology dynamics in healthy-toxic protein interaction and the multiscale analysis of neurodegenerative diseases. In: Paszynski, M., Kranzlmüller, D., Krzhizhanovskaya, V.V., Dongarra, J.J., Sloot, P.M.A. (eds.) ICCS 2021. LNCS, vol. 12746, pp. 528–540. Springer, Cham (2021). https://doi.org/10.1007/978-3-030-77977-1_42
16. Pekny, M., Michael, N.: Astrocyte activation and reactive gliosis. Glia **50**, 427–434 (2005)
17. Schäfer, A., et al.: Bayesian physics-based modeling of Tau propagation in Alzheimer's Disease. Front. Physiol. **12**, 702975 (2021)
18. Kerepesi, C., Szalkai, B., Varga, B., Grolmusz, V.: How to direct the edges of the connectomes: dynamics of the consensus connectomes and the development of the connections in the human brain. PLoS ONE **11**, e0158680 (2016)
19. Ossenkoppele, R., Rabinovici, G.D., Smith, R., Miller, B.L.: Discriminative Accuracy of [18F] flortaucipir positron emission tomography for Alzheimer Disease vs other neurodegenerative disorders. JAMA **320**, 1151–1162 (2018)